Research Paper

The Effect of Formulation Variables and Breathing Patterns on the Site of Nasal Deposition in an Anatomically Correct Model

Yang Guo,[1,3,4] Beth Laube,[2] and Richard Dalby[1]

Purpose. This study was conducted to evaluate the effect of formulation variables and breathing patterns on aerosol distribution in the nasal cavity.

Methods. Placebo nasal spray formulations containing 0.25% w/v Avicel CL611 (viscosity = 4 cP) and 2% w/v methylcellulose (MC; viscosity = 18.2 cP) were radiolabeled with ^{99m}Technicium. Following spraying into a silicone nose model, through which air was drawn at one of three constant rates (0, 10, and 20 L/min) or one of two breathing profiles (representing fast and slow inhalations), aerosol deposition in the model was quantified by gamma scintigraphy. Regional deposition was expressed as horizontal [inner, middle (h), outer] and vertical distribution [upper, middle (v), lower] in the nose model.

Results. Compared to 2% MC, Avicel CL611 significantly increased aerosol deposition in the middle (h) region of the nasal cavity under all breathing conditions, and in the inner region at 0 and 20 L/min and with a slow inhalation. The different breathing rates showed no effect on deposition of 2% MC. However, 10 L/min significantly increased the upper deposition of Avicel compared to 0 and 20 L/min.

Conclusions. Nasal sprays with a low viscosity provided greater surface coverage of the nasal mucosa than higher viscosity formulations. Changes in breathing profiles did not affect aerosol deposition in this nose model.

KEY WORDS: breathing pattern; deposition; formulation; gamma scintigraphy; nasal spray.

INTRODUCTION

Viscosity-enhancing polymers have been added to commercial nasal formulations to increase the retention time of medications in the nasal cavity, prevent dripping, and enhance the physical stability of suspended drugs (1). Commonly used polymers include microcrystalline cellulose (MCC), carboxymethylcellulose (CMC), and hydroxypropyl methylcellulose (HPMC).* In a preliminary study, we demonstrated that these polymers significantly changed the physical properties of bulk nasal formulations, as well as their plume shape and particle size distribution (2). Whether or not these formulation-induced changes in aerosol properties lead to altered deposition in the nasal cavity is the subject of the current investigation. Inconsistent results have been reported from previous studies. Harris and colleagues (1) added methylcellulose to a solution of desmopressin to increase its viscosity and assessed the distribution of the drug in the nasal cavity of healthy volunteers. Based on qualitative assessments of gamma camera images of the nasal cavity, they reported that distribution of the lower viscosity formulation was localized in the anterior region of the nasal cavity. No quantitative regional analyses were performed. Using a magnetic resonance imaging (MRI)-derived nose model, Cheng *et al.* (3) showed that larger droplets and a wider spray angle also increased deposition in the anterior region. However, Suman *et al.* (4) found that *in vitro* differences in the plume angle and spray pattern between two different nasal spray pumps spraying the same formulation did not lead to different deposition patterns in the nasal cavity of human volunteers. These observations raise questions about the usefulness of *in vitro* tests, such as plume geometry, spray pattern, and droplet size distribution, as surrogates for bioequivalence, as described in the latest FDA draft guidance documents (5). With such a limited body of knowledge in this area, we decided there was a significant need for quantifying the effect of formulation variables on deposition patterns of intranasally administered aerosols in a model system.

We were also interested in the influence of breathing rates and profiles on deposition site following use of a nasal spray pump. There is no consensus on the appropriate breathing rate or profile that a patient should attempt to achieve to elicit optimum nasal drug delivery [as evidenced by different instructions on package inserts and a lack of Food and Drug Administration (FDA) guidance on test conditions].

---

[1] Department of Pharmaceutical Sciences, University of Maryland at Baltimore, Baltimore, Maryland, USA.

[2] Department of Pediatrics, School of Medicine, The Johns Hopkins University, Baltimore, Maryland, USA.

[3] Present address: Schering Plough Research Institute, 2000 Galloping Hill Road, K-11-2 J5 Kenilworth, New Jersey, USA.

[4] To whom correspondence should be addressesd. (e-mail: yang.guo@spcorp.com)

* Nasacort AQ Nasal Spray (Sanofi-Aventis, Bridgewater, NJ, USA): microcrystalline cellulose and carboxymethylcellulose sodium. Dristan 12-h Nasal Spray (Wyeth Consumer Healthcare, Madison, NJ, USA): hydroxypropyl methylcellulose.

Ideally, these questions should be answered in clinical trials, during which possible correlations between formulation properties, aerodynamic performance, breathing patterns, and nasal deposition could be systematically investigated. However, clinical trials are expensive and time-consuming, especially as the number of study arms increases to encompass all the possible formulation variables. In addition, many formulations and novel excipients are not approved for human use during the development phase of the sprayed product. In an attempt to develop a model that could be used before clinical studies are undertaken, we quantified aerosol deposition of several formulations in the nasal passage of a silicone nose model derived from a human cadaver, using gamma scintigraphy and simulated breathing.

Results from these experiments are intended to fill the existing information gap (i.e., do changes in aerosol behavior and breathing profiles influence the site of nasal deposition?), facilitate industry moving forward with more confidence from *in vitro* product design concepts to performance verification during clinical trials, and provide a scientific basis on which manufacturers of nasal sprays can base their patient instructions.

METHODS AND MATERIALS

Nasal Formulations

A "high viscosity" 2% w/v methylcellulose (MC, Spectrum Chemicals and Laboratory Products, New Brunswick, NJ, USA; Lot Rg0975) and a "low viscosity" 0.25% w/v Avicel CL611 (FMC Corporation, Philadelphia, PA, USA; Lot E011N) nasal formulation was prepared in water. Test formulations did not contain any drug, surfactant, or preservatives.

Characterization of Physical Properties

Bulk viscosities were measured using a cone and plate Brookfield rheometer (Brookfield Engineering Laboratories, Middleboro, MA, USA) at 2 RPM after 2.5 min. Densities were determined by a DMA 48 density meter (Anton Paar GmbH, Graz, Austria). Surface tensions were measured by a Fisher Surface Tensiomat Model 21 with 6 cm platinum iridium ring. Three measurements per formulation were made at a temperature of 25°C.

Characterization of Aerosol Behaviors

Images of plume were captured by open-flash digital photography. Plume angle was analyzed using SigmaScan Pro (Jandel Scientific Software, San Rafael, CA, USA) to delineate the plume boundary based on optical density. Droplet size distribution was measured by laser diffraction using Spraytec (Malvern Instruments Inc, Southborough, MA, USA). Triplicate measurements were made for each formulation.

Anatomically Correct Model of Nasal Cavity

A single silicone nose model (Koken Co., Ltd., Tokyo, Japan) made from a healthy Japanese male cadaver head was used to quantify nasal deposition of the formulations described above. A stainless steel and Plexiglas clamp was custom-fabricated to hold the nose model in position for deposition studies within the gamma camera's field of view (Fig. 1).

Plexiglas and silicone were the only materials between the nasal cavity and the camera head. This design was adopted to minimize photon attenuation. The clamp ensured an airtight seal with the nose model, and the stainless steel side served as the nasal septum and provided an attachment point for a vacuum source that could pull air through the model to simulate an inhalation. Prior to use, the model was flooded with Dawn concentrated dish liquid detergent (Procter & Gamble, Cincinnati, OH, USA) and acetone (Fisher Scientific, Fair Lawn, NJ, USA; Lot 981540, 10:4 ratio by volume), drained, and allowed to air-dry. This coating procedure was used to impose an aqueous "nasal mucosa" on the otherwise hydrophobic silicone of the model. Preliminary experiments showed this minimized reentrainment, migration, and dripping of impacted aqueous droplets. The nostril opening was enlarged slightly to accept the tip of the nasal spray pump without producing an airtight seal.

Deposition Studies in the Anatomically Correct Nose model

Nose Reference Scan

The nose model was flooded with 30 mL ethanol admixed with 20 μCi ^{99m}technetitum (^{99m}NaTcO$_4$; Cardinal Health, Baltimore, MD, USA). The model in its clamp was placed at a predetermined position in front of a ZLC 370 gamma camera (Siemens Gammasonics, Inc., Des Plaines, IL, USA). A scintigraphic image was acquired by the gamma camera for 6 min with the region between nasopharynx and pharynx of the nose model blocked by a piece of lead as shown in Fig. 2. The functional borders of the nasal cavity from nasal
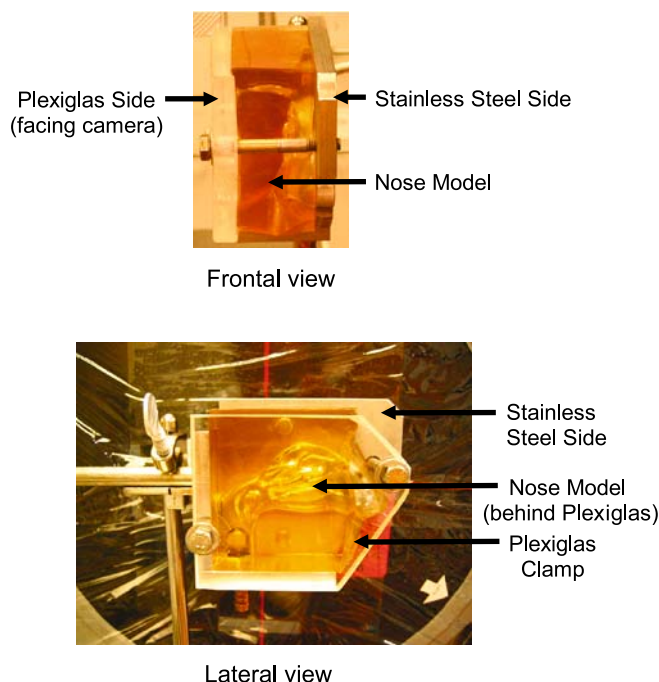

Plexiglas Side (facing camera)
Stainless Steel Side
Nose Model

Frontal view

Stainless Steel Side
Nose Model (behind Plexiglas)
Plexiglas Clamp

Lateral view

Fig. 1. Silicone nose model with stainless steel and Plexiglas clamp.

Ethanol, 20 uCi ^{99m}Tc

lead

Region behind
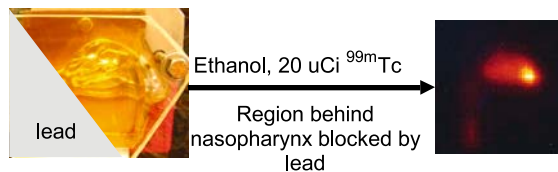nasopharynx blocked by
lead

Fig. 2. Defining the border of the nasal cavity with the nasopharynx blocked by lead shielding.

vestibule to nasaopharynx were then identified on the gamma camera image (and subsequently referred to as the "nose reference scan"). In addition, these images document the absence of leaks.

Formulation Preparation for Deposition Study

^{99m}Tc (400 µCi) was added to 2 mL of each test nasal formulation and the mixture was filled into a screw-top glass bottle, fitted with a 100 µL per actuation pump taken from Afrin® No Drip (Schering-Plough HealthCare Products Inc., Memphis, TN, USA). The target dose of radionuclide was 20 µCi per actuation. To minimize operator-induced variation, an automated actuation station (InnovaSystems, Pennsauken, NJ, USA) was used to release sprays with a constant actuation force of 4.5 kg. Each formulation was primed five times before the shot weight and unit radioactive dose were measured on the sixth spray. The radioactivity was quantified by a dose calibrator (Capintec, Inc., Ramsey, NJ, USA).

Collection of Breathing Profiles

Instrument: The apparatus (Fig. 3) was modified from a breath recording system developed in our laboratory (6). It consisted of a face mask (GM Instruments Ltd., Kilwinning, UK), a pneumotachograph (GM Instruments), a differential pressure transducer (OMEGA, Stamford, CT, USA), a data acquisition card (DAQ card 1200, National Instruments, Austin, TX, USA) that communicated with a computer via a C language program. This system records the instantaneous flow rate every 100 ms.

Subjects: Nasal breathing profiles were recorded from nine healthy volunteers (three males and six females) via the instrumented face mask. Volunteers were between the ages of 20 and 40, and reported no more than occasional prior
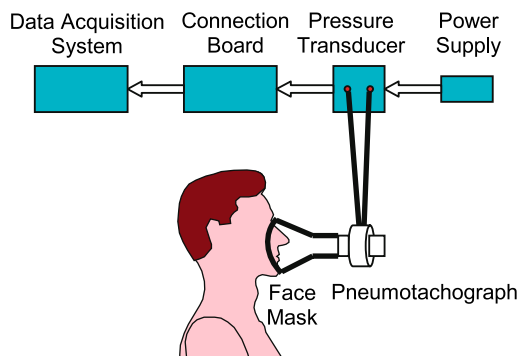
use of nasal sprays. The test was performed when the subjects were in the sitting position breathing ambient air. The left nostril of each volunteer was blocked by a piece of tape over the exterior nares. We captured "slow" and "fast" breathing profiles (representing the extremes of nasal inhalation behavior), by randomly asking volunteers to "breathe gently through your nose with your mouth closed" or to "breathe vigorously through your nose with your mouth closed"), and recording the result.Breathing profiles collected from healthy volunteers were evaluated with regard to inhaled volume, peak inspiratory flow rate (PIF), time to reach PIF (T_{max}), inhalation duration (T_d), and the slope of the initial inspiratory flow rate *vs.* time curve. Inhaled volumes were determined by integration of the area under the curve. Based on these parameters, simplified breathing profiles with a trapezoidal shape were designed by approaching the mean peak inspiratory flow rate using the mean linear initial slope, and then maintaining the mean PIF until the mean inhaled volume was reached. The end of the inhalation was defined by a linear drop to zero flow over a 100-ms interval.

Breathing Simulation

An updated breathing simulation system was built on the chassis of an older unit developed in our laboratory (6). This system had two major functions: (1) to generate target breathing profiles, and (2) to simultaneously verify attainment of the target breathing profile. A schematic diagram of the breathing simulation system is shown in Fig. 4.

While a vacuum pump generated a constant negative pressure, airflow rate through the nose was controlled by the opening of an electrical flow control valve (Teknocraft Inc., Melbourne, FL). A custom program in Labview 7.1 (National Instruments) precisely controlled opening of the valve via a DAQ card based on stored breathing profiles. The instantaneous flow rate of breathing profiles generated in this way were simultaneously recorded by the same DAQ card via a pneumotachograph (GM Instruments) and pressure transducer (OMEGA). Results retrieved from the DAQ card were displayed, analyzed, and archived by the computer software.

Deposition Study in the Nose model

The assembled equipment is shown in Fig. 5. The nose model and Plexiglas section of the clamp were transparent to
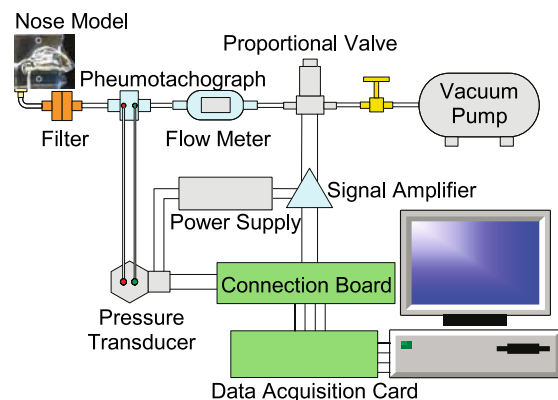

Data Acquisition System   Connection Board   Pressure Transducer   Power Supply

Face Mask   Pneumotachograph

Fig. 3. Breath recording system consisted of a face mask, a pneumotachograph, a pressure transducer, and a data acquisition card that communicated with a computer.

Nose Model

Proportional Valve

Pheumotachograph

Vacuum Pump

Filter   Flow Meter

Signal Amplifier

Power Supply

Connection Board

Pressure Transducer

Data Acquisition Card

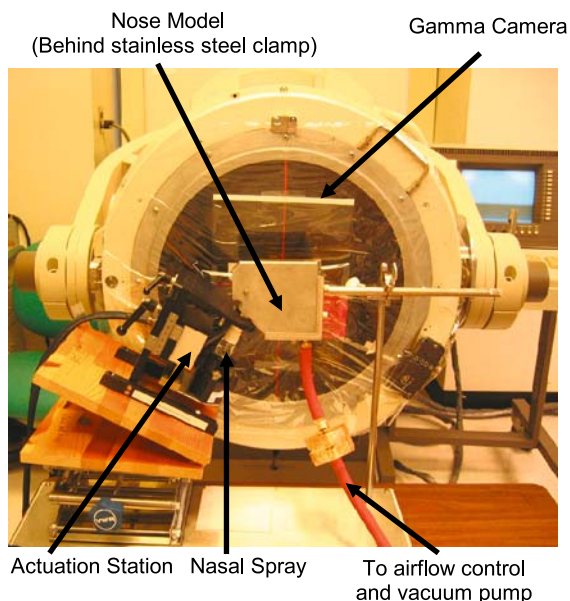**Fig. 4.** Block diagram of breathing simulator.

Fig. 5. Equipment for nasal deposition study with gamma scintigraphy. The gamma camera head is the round circular structure. The nose model is invisible, but is positioned behind the rectangular stainless steel clamp centered directly in front of the gamma camera. Nasal spray pump was inserted 1 cm into the nose model through the nostril opening. Spray was actuated using an automated actuation station. Airflow was drawn through the bottom of the nose model by a vacuum pump and control system. A filter was placed between the nose model and the vacuum pump to collect any radioactive dose that bypassed the nose model.

gamma emissions, so scintigraphic deposition images could be reconstructed from detection of the origin of these emissions in the model using a gamma camera and computer. The nose model was positioned in front of the gamma camera to ensure alignment of the nose reference scan and radioaerosol scintigrams. The outer lateral side of the nose model was placed as closely as possible against the head of the gamma camera to decrease attenuation. A vacuum pump drew airflow through the nose model from the nostril to the nasopharynx.
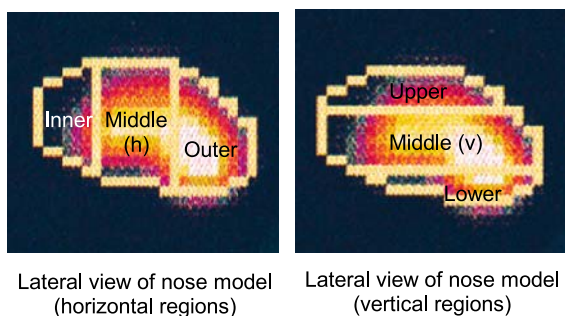

Fig. 6. Quantifying nasal deposition. The region outlined in yellow represents the nasal cavity, which was divided into three regions, vertically and horizontally. The red and white areas represent the aerosol image. White indicates areas with the highest radioactivity, whereas black indicates no radioactivity was present. Inner and outer zones represent the anterior and posterior regions of the nasal cavity, respectively. The upper zone depicts the superior areas, which include the olfactory region, and the lower zone denotes the floor of the nasal cavity and inferior turbinate.

Table I. Physical and Spray Properties of 0.25% Avicel CL611 and 2% MC

	0.25% Avicel	2% MC
Viscosity (cP)	4.0 ± 0.2^a	18.2 ± 0.9
Density (g/cm^3)	1.0 ± 0	1.0 ± 0
Surface tension (dyn/cm)	77.3 ± 0.7	60.0 ± 1.3
Plume Angle (°)^b	68.7 ± 0.4	32.5 ± 0.5
Dv_{10} (μm)^b	17.2 ± 0.2	97.5 ± 3.0
Dv_{50} (μm)^b	37.7 ± 0.3	198.7 ± 8.8
Dv_{90} (μm)^b	85.3 ± 0.8	305.0 ± 18.0

[a] Results are expressed as mean $\pm$ SD ($n = 3$).
[b] Plume angle, Dv_{10} (10% of the cumulative volume undersize), Dv_{50} (volume median diameter), and Dv_{90} (90% of the cumulative volume undersize) are cited from a previous study (1).

Three constant airflow rates of 0, 10, or 20 L/min and two simulated breathing profiles (fast and slow inhalation, as described previously) were studied. A filter was placed between the nose model and vacuum pump to collect any radioactive droplets that bypassed the nose model (i.e., those that did not deposit). Radioactivity on the filter was quantified by a dose calibrator (Capintec, Inc.) after nasal deposition. Whereas the test air flow rate or profile was drawn through the nose model, one spray of nasal formulation admixed with the radioisotope ^{99m}Tc was automatically administered into the nostril using the automated actuation station. Actuation was coordinated with the onset of the inhalation when the profiles were studied. After the profile was completed or the airflow stopped, the nasal spray bottle and actuation station were immediately removed and placed behind a lead shield to avoid masking and scattering effects caused by the high radioactivity remaining in the nasal spray bottle. Then, a lateral view of the nasal cavity was acquired by the gamma camera for 2 min. Following completion of the first radioaerosol image scan, two more 2-min images were acquired to detect postdeposition migration of aerosol within the nose model over time. Camera sensitivity was calibrated before each experiment using a 100-μCi ^{99m}Tc source.

Regions of interest were identified on the nose reference scan and covered the region between nasal vestibule and nasopharynx. These regions were superimposed on subsequent radioaerosol images (Fig. 6). During computer processing, the radiolabeled image was registered with the nose reference image. Data were analyzed in terms of horizontal and vertical distribution. Regional deposition in the horizontal direction was quantified in terms of radioactivity deposited

Table II. Inhalation Parameters Derived from Each Breathing Pattern

Breathing pattern	Tidal volume (mL)	PIF (L/min)	T_{max} (s)	T_d (s)	Slope (L/min s)
RS^a	560.6 ± 260.3	20.2 ± 8.0	0.4 ± 0.5	1.9 ± 1.0	50.9 ± 29.9
RF^a	619.1 ± 517.7	35.8 ± 14.1	0.3 ± 0.4	1.2 ± 0.6	133.6 ± 61.3

[a] RS represents right nostril, slow inhalation. RF represents right nostril, fast inhalation. All values are expressed as mean $\pm$ standard deviation of the mean ($n = 9$).
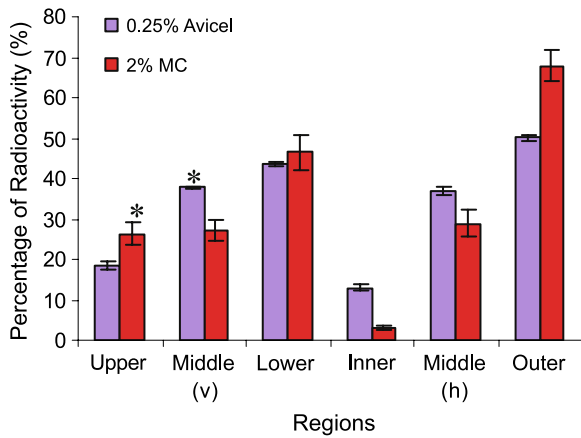
Fig. 7. Effect of formulation properties on the nasal deposition pattern at 0 L/min. Error bars represent standard deviation ($n = 3$). *$P < 0.05$.

Table IV. Regional Distribution of 2% MC with Changing Breathing Rates and Profiles

| Regions | Percentage of Radioactivity (%)[a] | | | | |
	0 (L/min)	10 (L/min)	20 (L/min)	Slow inhalation	Fast inhalation
Upper	26 ± 3^b	24 ± 10	27 ± 10	34 ± 3	32 ± 5
Middle (vertical)	27 ± 3	31 ± 4	28 ± 2	33 ± 1	32 ± 1
Lower	46 ± 5	45 ± 8	45 ± 12	33 ± 4	36 ± 6
Inner	3 ± 0	10 ± 8	2 ± 0	2 ± 0	2 ± 0
Middle (horizontal)	29 ± 4	31 ± 13	21 ± 5	25 ± 1	25 ± 3
Outer	68 ± 4	59 ± 20	77 ± 5	73 ± 1	72 ± 3

[a] Percentage of radioactivity = $100 \times \frac{counts(local)/pixel(local)/min}{counts(overall)/pixel(overall)/min}$.
[b] Results are expressed as mean $\pm$ SD ($n = 3$).

in an inner, middle (h), and outer region. Regional deposition in the vertical direction was quantified in terms of radioactivity deposited in an upper, middle (v), and lower region of the nasal cavity for all the lateral nasal cavity images. Radioactivity in the nasal cavity was calculated on the basis of counts collected over 2 min in single views after subtraction of background radioactivity and correction for radioactive decay to the time of administration. Mean counts per pixel per minute in each of the regions described above were calculated. Regional distribution was expressed as percentages of the mean counts per pixel per minute in the nose model. Three measurements were made for each formulation.

Statistical Analysis

All data are presented as mean ± standard deviation (SD). A Kruskal–Wallis one-way analysis of variance test was used to identify significant differences in upper, middle (v), lower, inner, middle (h), and outer deposition for the two formulations at the three breathing rates and two breathing profiles. A Mann–Whitney rank test (two-tail) was also used to determine significant differences between regional distribution for each formulation at the three breathing rates and

the two breathing profiles. These nonparametric tests were used because they do not require any assumption of normal distribution, and were most appropriate for our small sample size. P values less than 0.05 were judged to represent significant differences.

RESULTS

Physical Properties

The physical properties and aerodynamic behaviors of 0.25% Avicel CL611 and 2% MC are summarized in Table I.

Nasal Breathing Profiles Based on Healthy Volunteers

The measured breathing profiles from all nine volunteers who engaged in the "fast" and "slow" inhalations through their right nostril were evaluated with regard to inhaled volume, peak inspiratory flow rate (PIF), time to reach PIF (T_{max}), inhalation duration (T_d), and the slope of the initial inspiratory flow rate $vs.$ time curve. Average breathing parameters are shown in Table II.
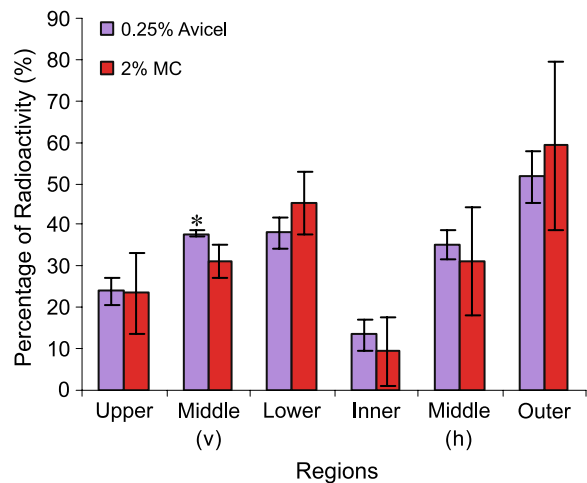

Fig. 8. Effect of formulation properties on the nasal deposition pattern with 10 L/min. Error bars represent standard deviation ($n = 3$). *$P < 0.05$.
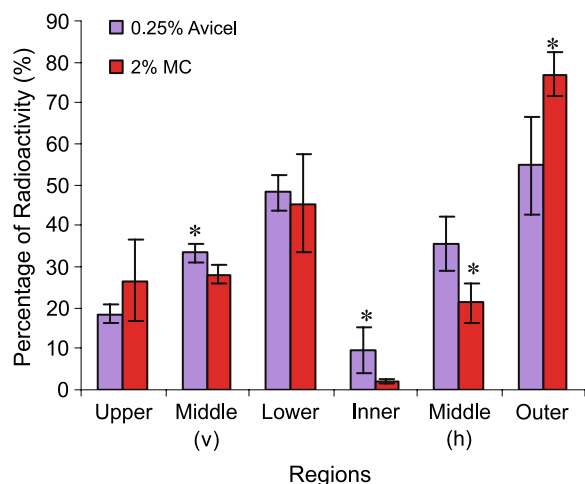
Table III. Regional Distribution of 0.25% Avicel CL611 with Changing Breathing Rates and Profiles

| Regions | Percentage of radioactivity (%)[a] | | | | |
	0 (L/min)	10 (L/min)	20 (L/min)	Slow inhalation	Fast inhalation
Upper	19 ± 1^b	24 ± 3	18 ± 2	21 ± 2	23 ± 1
Middle (vertical)	38 ± 0	38 ± 1	33 ± 2	37 ± 1	37 ± 1
Lower	44 ± 1	38 ± 4	48 ± 4	42 ± 3	40 ± 2
Inner	13 ± 1	13 ± 4	10 ± 6	11 ± 4	8 ± 8
Middle (horizontal)	37 ± 1	35 ± 4	36 ± 7	38 ± 2	32 ± 6
Outer	50 ± 1	52 ± 6	55 ± 12	51 ± 6	60 ± 10

[a] Percentage of Radioactivity = $100 \times \frac{counts(local)/pixel(local)/min}{counts(overall)/pixel(overall)/min}$.
[b] Results are expressed as mean $\pm$ SD ($n = 3$).

Fig. 9. Effect of formulation properties on the nasal deposition pattern with 20 L/min. Error bars represent standard deviation ($n = 3$). *$P < 0.05$.

Deposition Study

Nasal deposition data are derived from the first 2-min image acquisition from both formulations tested in the nose model at three constant airflow rates (0, 10, and 20 L/min) and two simulated breathing techniques (fast and slow). Deposition data from the second and third 2-min images acquisitions were similar to data for the first 2-min image, indicating no postdeposition migration of aerosol within the nose model over a 6-min period. No radioactivity was detected on the filter between the vacuum and nasal cast.

Effect of Formulation Properties on Nasal Deposition

At 0 L/min (Fig. 7). Compared to 2% MC, 0.25% Avicel CL611 significantly decreased the percentage of radioactivity in the upper region from 26 to 19% ($p = 0.046$), and significantly increased deposition in the middle (v) region from 27 to 38% ($p = 0.034$), in the inner region from 3 to 13% ($p = 0.043$) (Tables III and IV). No other significant regional differences were observed between the two formulations.
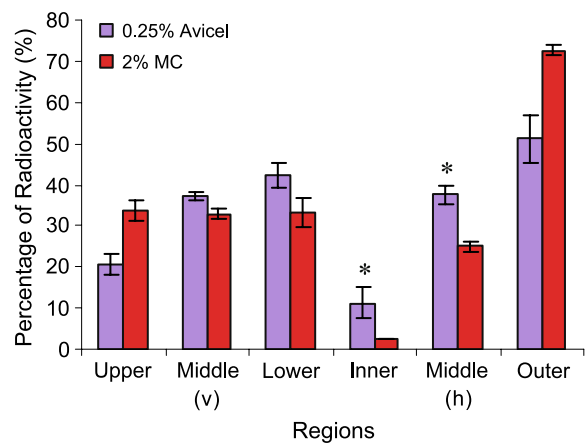

Fig. 10. Effect of formulation properties on the nasal deposition pattern with slow inhalation. Error bars represent standard deviation ($n = 3$). *$P < 0.05$.
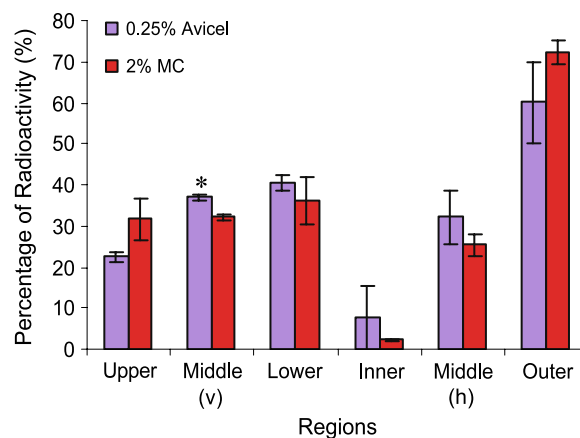

Fig. 11. Effect of formulation properties on the nasal deposition pattern with fast inhalation. Error bars represent standard deviation ($n = 3$). *$P < 0.05$.

At 10 L/min (Fig. 8). Compared to 2% MC, 0.25% Avicel CL611 significantly increased the percentage of radioactivity in the middle (v) region from 31 to 38% ($p = 0.003$). No other significant regional differences were observed between the two formulations ($p > 0.05$).

At 20 L/min (Fig. 9). Compared to 2% MC, 0.25% Avicel CL611 significantly increased the percentage of radioactivity in the middle (v) region from 28 to 33%, in the inner region from 2 to 10%, in the middle (h) region from 21 to 36%, and significantly decreased deposition in the outer region from 77 to 55% (all $p < 0.05$). No other significant regional differences were observed between the two formulations ($p > 0.05$).

Simulated slow breathing (Fig. 10). Compared to 2% MC, 0.25% Avicel CL611 significantly increased the percentage of radioactivity in the inner region from 2 to 11% ($p = 0.043$), and increased deposition in the middle (h) region from 25 to 38% ($p = 0.046$). No other significant regional differences were observed between the two formulations ($p > 0.05$).

Simulated fast breathing (Fig. 11). Compared to 2% MC, 0.25% Avicel CL611 significantly increased the percentage of radioactivity in the middle (v) region from 32 to 37% ($p = 0.046$). No other significant regional differences were observed between the two formulations ($p > 0.05$).
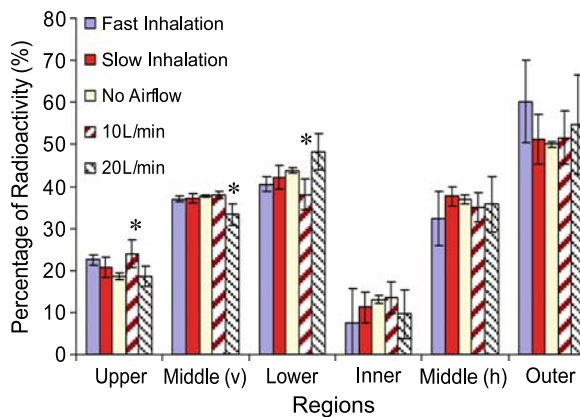

Fig. 12. Effect of breathing patterns on the nasal deposition pattern of 0.25% Avicel CL611. Error bars represent standard deviation ($n = 3$). *$P < 0.05$.
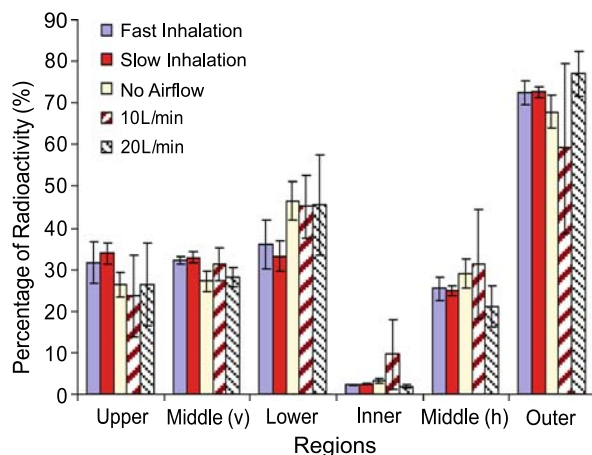
Fig. 13. Effect of breathing patterns on the nasal deposition pattern of 2% MC. Error bars represent standard deviation ($n = 3$).

Effect of Breathing Rates on Nasal Deposition of 0.25% Avicel CL-611 and 2% MC

As shown in Fig. 12, for 0.25% Avicel CL-611, breathing rates affected the vertical, but not the horizontal distribution (Tables III and IV). For the upper region, deposition was highest at 10 L/min compared to 0 or 20 L/min ($p < 0.05$). For the middle (v) region, deposition was lowest at 20 L/min compared to 0 or 10 L/min ($p < 0.05$). For the lower region (38%), deposition was lowest at 10 L/min compared to 0 and 20 L/min ($p < 0.05$).

As shown in Fig. 13, for 2% MC, no significant differences were observed in the regional aerosol distributions (horizontal or vertical) for the three breathing rates (0, 10, and 20 L/min) tested (all $p > 0.05$).

Effect of Simulated Breathing on Nasal Deposition of 0.25% Avicel CL-611 and 2% MC

Comparing the two formulations, the two breathing profiles showed no significant effect on horizontal or vertical aerosol distribution (all $p > 0.05$) (Tables III and IV). For 0.25% Avicel CL611 (Fig. 12), a comparison of regional deposition (horizontal and vertical) at the three breathing rates (0, 10, and 20 L/min) and the two breathing profiles showed a significant decrease in middle (v) deposition at 20 L/min (all $p < 0.05$). No significant regional differences were observed for 2% MC (Fig. 13) for the breathing rates or breathing profiles.

DISCUSSION

These data suggest that the low viscosity formulation, 0.25% Avicel CL611, significantly enhanced middle and posterior (inner region) coverage of the nasal cavity compared to the higher viscosity formulation, 2% microcrystalline cellulose, at 0 and 20 L/min, and with a slow inhalation. The increased surface coverage of the low viscosity formulation may be attributed to the production of smaller droplets ($Dv_{50} = 37.7 \pm 0.3$ µm) sprayed at a wider plume angle ($68.7 \pm 0.4°$). It is also possible that the smallest droplets were more readily entrained by the inhaled air stream, and were

subsequently carried deeper into the nose. In the case of the high viscosity formulation, the resulting aerosol droplets would be more resistant to directional changes due to increased inertia attributable to their large droplet size ($Dv_{50} = 198.7 \pm 8.8$ µm). As a result, the large droplets probably maintained their original direction of travel leaving the nozzle and impacted on the first oblique surface they encountered by inertial impaction. This led to deposition in the front of the nose. This study provides some justification for the FDA's requirements that innovator and generic nasal spray products remain qualitatively and quantitatively similar to avoid depositing in different regions of the nose. Nevertheless, the clinical implications of the different deposition patterns remain uncertain. In addition, the middle section of the nasal cavity (also called the respiratory region) is considered to represent the optimal area for drug absorption, because of plentiful blood flow and a large surface area (7). A low viscosity formulation may therefore favor the absorption of a pharmaceutical compound by delivering the drug toward the middle and posterior regions of the nasal cavity.

When compared to Avicel, the higher viscosity formulation (2% MC) did not evoke a significant change in the nasal distribution of the sprayed droplets at the different airflow rates or breathing profiles. For the low viscosity formulation (0.25% Avicel CL611), a constant airflow of 10 L/min significantly increased the surface coverage in the upper region (near olfactory region) when compared to 0 and 20 L/min. However, there was no difference in regional deposition with slow *vs.* fast breathing profiles. In contrast, 20 L/min led to a significant reduction of deposition in the middle region (vertical) compared to the other breathing rates and profiles tested. This reversal in deposition could involve the following explanation. An airflow rate of 10 L/min may have increased the upward travel of droplets before gravity caused them to fall to the floor of the nasal cavity. Further increase in airflow rate (i.e., 20 L/min) may have induced turbulence, and dragged the droplets in unpredictable directions. The increased surface coverage of the upper region with Avicel at 10 L/min indicates that this airflow rate and formulation might favor drug delivery to the olfactory region and possibly central nervous system (CNS) delivery. The reduced surface coverage of the middle region (the major site of drug absorption in the nasal cavity) at 20 L/min suggests this flow rate may be less desirable for efficient nasal drug delivery.

When tested with fast and slow breathing profiles, regional distributions (vertical or horizontal) of these two formulations were not significantly different. The initially high velocity and mass of the droplets exiting the spray nozzle probably ensured they had sufficient momentum to impact on the first surface directly in their path (generally very close to their point of release in the nose), irrespective of the air flow rate into which they were introduced. Although it is interesting to speculate that smaller droplets are those that reach the upper regions of the nose, and are the most susceptible to imposed airflow, these data provide no such confirmation.

Similar aerosol distributions in the nose model with fast and slow breathing profiles were consistent with a clinical study conducted by Newman *et al.* (8), in which gentle and vigorous sniff showed no effect on nasal deposition of an insulin nasal spray. This indicates that there does not seem to

be a reason for the various breathing instructions given to patients by different manufacturers of nasal spray products. A patient who mixes up his or her breathing instructions when using two products of similar composition would be unlikely to experience variability in their deposition pattern and may have needlessly worried about learning two different breathing techniques. Based on our data, we believe it would be appropriate to develop a uniform set of instructions for using a nasal spray to minimize patient confusion.

Because the influence of both formulation and breathing rates in this study were subtle, it is unlikely they could have been detected at all in a clinical study in patients or volunteers against the background of intersubject variability. Clearly, nasal deposition studies with nose model and simulated breathing do not provide a surrogate for clinical studies, but, in the absence of such studies, do provide additional guidance to formulators, or those designing package inserts or clinical trials of nasal products.

Postmortem shrinkage due to desiccation of tissues, or shrinkage of casting polymers during curing is a known problem associated with the development of airway models. However, as the model was used on the assumption that it was in some way representative of a typical human nose, it is not critical that it be an accurate model of a specific nose. Our findings are general in nature and it is unlikely that the trends we report would be altered by small dimensional differences.

CONCLUSIONS

Low viscosity nasal spray formulations seem to enhance deposition distal to the nares compared to higher viscosity formulations. Constant breathing rates produced some differences in nasal spray deposition. However, we did not observe any effect of breathing profiles (that are more likely to represent the breathing conditions of patients using their nasal sprays) on deposition in this *in vitro* model in conjunction with two formulations representing the extremes of viscosity. For this reason, we believe it might be appropriate to develop a uniform set of instructions for using a nasal spray to minimize patient confusion.

ACKNOWLEDGMENTS

REFERENCES

1. A. S. Harris, E. Svensson, Z. G. Wagner, S. Lethagen, and I. M. Nilsson. Effect of viscosity on particle size, deposition, and clearance of nasal delivery systems containing desmopressin. *J. Pharm. Sci.* **77**(5):405–408 (1988).
2. Y. Guo. *Improving nasal drug delivery—investigation of the effect of formulation variables on in vitro performance of nasal sprays*. Dissertation, University of Maryland, Baltimore, 2005.
3. Y. S. Cheng, T. D. Holmes, J. Gao, R. A. Guilmette, S. Li, Y. Surakitbanharn, and C. Rowlings. Characterization of nasal spray pumps and deposition pattern in a replica of the human nasal airway. *J. Aerosol Med.* **14**(2):267–280 (2001).
4. J. D. Suman, B. L. Laube, T. Lin, G. Brouet, and R. Dalby. Validity of *in vitro* tests on aqueous spray pumps as surrogates for nasal deposition. *Pharm. Res.* **19**:1–6 (2002).
5. Food Drug Administration. *U.S. FDA Draft Guidance for Industry: Bioavailability and Bioequivalence Studies for Nasal Aerosols and Nasal Sprays for Local Action*, US Food and Drug Administration, Washington, DC, 2003.
6. Z. Li. *Development of a patient inhalation training tool of simulated inhalations to study dry power inhaler performance realistically in vitro*. Doctoral dissertation, University of Maryland, 2002.
7. P. Arora, S. Sharma, and S. Garg. Permeability issues in nasal drug delivery. *DDT* **7**(18):967–975 (2002).
8. S. P. Newman, K. P. Steed, J. G. Hardy, I. R. Wilding, G. Hooper, and R. A. Sparrow. The distribution of an intranasal insulin formulation in healthy volunteers: effect of different administration techniques. *J. Pharm. Pharmacol.* **46**:657–660 (1994).